Fully Differential 2 GHz 2.7V 4th-Order Low-Noise Active Bandpass Filter on Silicon

Zoheir Sassi[1], Bruno Barelaud[1], Laurent Billonnet[1], Bernard Jarry[1],
Hervé Marie[2], Alain De La Torre[2], Nguyen Trieu Luan Le[2], Patrice Gamand[2]

[1] IRCOM, University of Limoges, 123 Avenue Albert Thomas, 87060 Limoges Cedex, France
[2] Innovation Centre RF, Philips Semiconductors, 2 rue de la girafe, 14079 Caen Cedex, France
E-mail: zoheir.sassi@unilim.fr

***Abstract* — In this paper we present a 2.7 V fully differential fourth-order bandpass filter developed and realised around four inductors electrically coupled using MOSFETs. Varactors are used for frequency tuning. An amplifier is cascaded at the input for noise and impedance matching. Philips QUBIC4 Si BiCMOS technology is used [1].**

I. Introduction

Nowadays, RFIC researchers are looking for new microwave topologies using the cheapest available technologies to get best performances in terms of size and power consumption at low cost. Many attempts have been done to perform the best-integrated solutions of RF front-ends in terms of optimised gain, noise and linearity [2-7].

The proposed topology in this paper is a 2.7 V 2 GHz fourth-order LC bandpass filter based on an emulation of magnetically coupled resonators [2][4]. The whole circuit occupies an area of 0.917 mm^2 and performs a gain of 34 dB with a 43 MHz bandwidth. The filter consumption is 5.5 mA/pole (i.e. 59 mW). With buffering and input amplification, total power consumption ends up to 32 mA (i.e. 86 mW). The circuit performs a noise figure of 4.4 dB, an input compression point of P-1dB=-7 dBm, and a dynamic range of 82.5 dB.

II. Circuit Architecture

Based on [2] and [4], we have designed a 2 GHz fourth-order LC differential bandpass filter based on magnetically coupled inductors. The lossy LC tanks are characterised by the inductor series resistance Ri and linked through a coupling coefficient k as shown in Fig.1. Ri includes also the resistive terminations of the g_{in} and g_{out} differential transconductances used for matching.

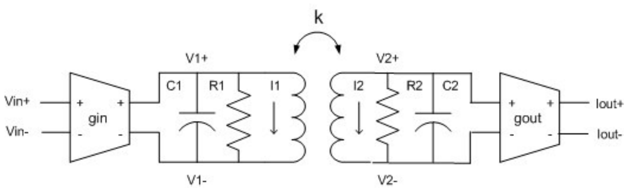

Fig. 1 Magnetically coupled LC tank based circuit

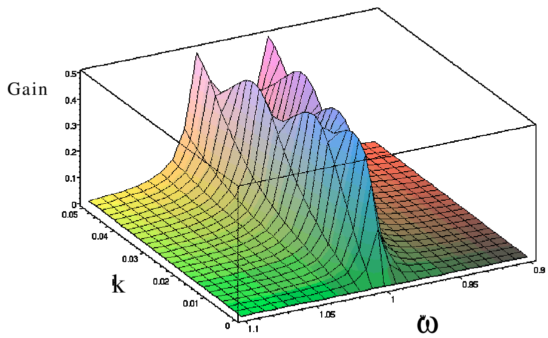

Fig. 2 Frequency response of the magnetically coupled tank circuits with respect to k

This way of coupling the two LC circuits leads to a frequency response depending on the coupling coefficient k like shown in Fig-2.

Considering that the two LC tanks are identical, the global circuit is governed by the following 4th-order expression (1):

$$\frac{I_{out}}{V_{in}} = \frac{g_{out} g_{in} sLk}{\left(1 + s\frac{L}{R} + s^2 LC\right)^2 - k^2} \tag{1}$$

The circuit resonates at frequency ω_0 (2) with a quality factor Q. Depending on the coupling coefficient k (3) and resistive terminations R (4), a selective response at a critical coupling can be obtained with a minimum ripple. K_1, K_2 constants depend on the number of resonators and on the critical coupling conditions. Δf is the frequency bandwidth of the filter [2][8].

$$K_1 = 1/\sqrt{2} \qquad K_2 = \sqrt{2}$$

$$\omega_0 = \sqrt{1/LC} \tag{2}$$

$$k = K_1\left(\Delta f / f_0\right) \tag{3}$$

$$R = R_1 = R_2 = K_2 Q \sqrt{L/C} \tag{4}$$

Following the same idea, coupling can be done electrically using MOSFETs (Fig.3).

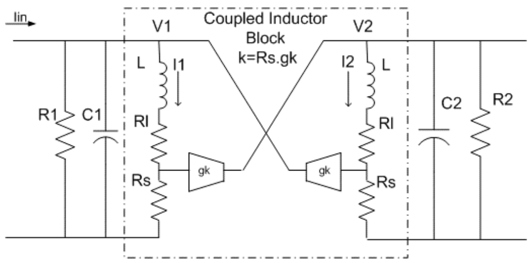

Fig. 3 Electrical coupling topology

In this circuit, coupling coefficient k is controlled by the resistor Rs. Its value directly drives the gate voltage of the transistor. The MOSFET transconductance gk is chosen to obtain k = Rs.gk with Rs = 5.3Ω. This value is a compromise between noise and power consuming.

Compensating negative resistances were added at the input and output of the circuit (Fig. 4) to reduce the total resistance Rt = Rs + Rl [3][4]. The final topology expression is (5) [2]:

$$\frac{V_2}{V_{in}} \approx -\frac{k}{\left(1+{R_t}/{R}\right)^2}\,\frac{g_{in}\left(R_t+sL\right)}{\left[1+s\left[\sqrt{1+\frac{R_t}{R}K_2Q\omega_0}\right]^{-1}+\frac{s^2}{\omega_0^2}\right]^2} \qquad (5)$$

where k is estimated to be very small than unity.

$\omega_0 = \frac{1+gRt}{LC}$ is the resonance frequency in that case.

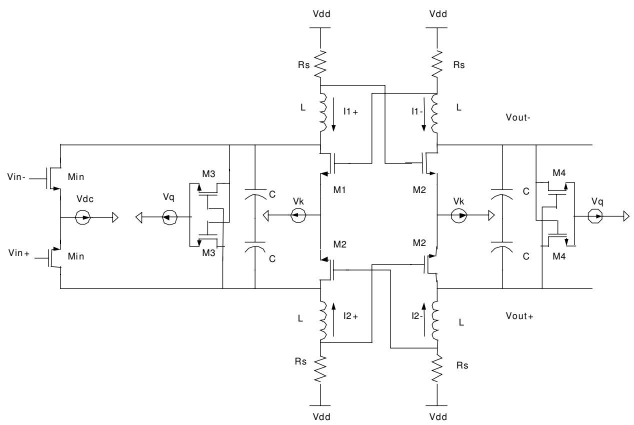

Fig.4 Simplified differential compensated filter circuit.

III. Inductor Modelling

The inductor block has 8 ports as shown in Fig. 6. It is constituted of four inductors L1 to L4 mutually induced by a coefficient k. These four inductors are spaced of 92 µm from each other. Each inductor is composed of 7 turns of 64 µm x 64 µm and constituted by three layers in series M6-M5-M3. The four inductor block is modelled using Momentum software. Pi models were used for each inductor and magnetic coupling coefficient is considered between them.

Each inductor performs the following values : L=2.9 nH, R=8.1 Ω (series resistance), C1=112.6 pH (input substrate capacitor), R1=2.28 kΩ (input substrate resistance), C2=196.9 pH (output substrate capacitor), R2=0.81 kΩ(output substrate resistance). LC tank block is the smallest and most important part (less than 6% of the whole area, with 224 µm x 224 µm – see Fig. 5).

IV. Circuit Layout

Circuit dimensions are 1030 µmx890 µm corresponding to a 0.917 mm² area. The most important area is used by the two input matching inductors (300 µm x 300 µm each, 20 % the total surface) (Fig. 5).

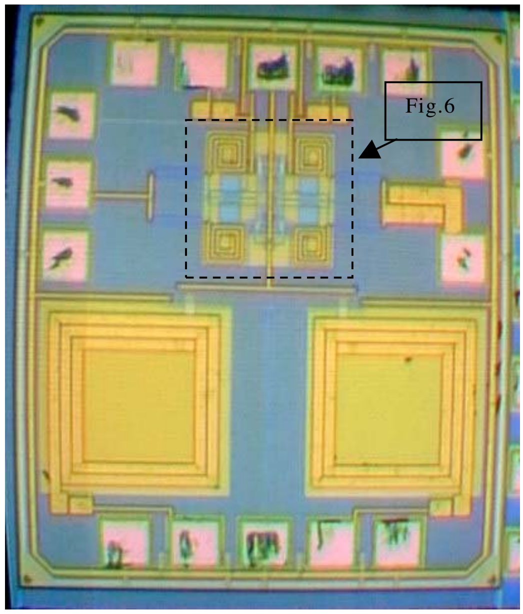

Fig. 5 Complete filter Photomicrography

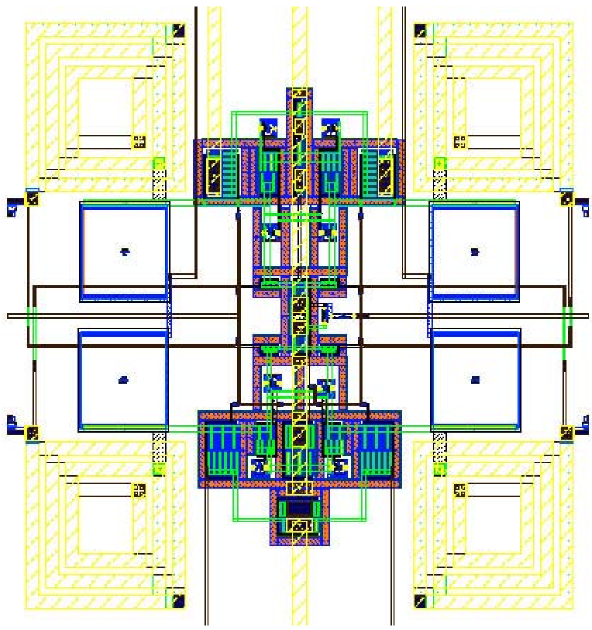

Fig. 6 Eight-port inductors block layout

	[5]	[6]	[2]	This work
Filter order	4			
f_0 (GHz)	0.85	1.9	1.8	2.05
Δf_{-3dB} (MHz) bandwidth	18	150	80	43
Passband Gain S21 (dB)	0	0	9	34
Ripple in passband (dB)	<±1	+1.6	<±0.25	<±0.25
Output P_{-1dB} (dBm)	-18	/	-40	-41 (total circuit)
Power consuming /pole mA	19.25	4.5	4	5.5 (Total of 32 mA)
Technology	0.8µm CMOS	0.25µm BiCMOS	0.5µm CMOS	0.25µm BiCMOS
Area/pole (mm^2)	0.5	0.25	.0585	0.229 (total of 0.917)
Supply voltage	2.7V			
Dynamic Range	61 dB	63 dB	42 dB	82.5 dB
Noise Figure	/	/	/	4.4 dB

Tab. 1 Comparison with similar circuits using the same topology

V. COMPARISON RESULTS AND CONCLUSION

Using baluns, our filter performs a gain of 34 dB at 2.05 GHz, with a –3dB bandwidth of 43 MHz and a noise figure of 4.4 dB as shown in Fig. 7 and Fig. 8. Input and output matchings are respectively -21.73 dB and -16 dB. Power consumption is 32 mW, with a -1dB output compression point of P-1dB = -7dBm. Referring to Tab. 1, many advantages can be noticed in comparison to former similar topologies. Matched to 50 Ω at both ports, the circuit shows an acceptable noise figure with respect to its narrow bandwidth and a better dynamic range of 82.5 dB. This latter is computed as the ratio of the -1dB compression output power (-41dBm) to noise output power of (– 123.5dBm).

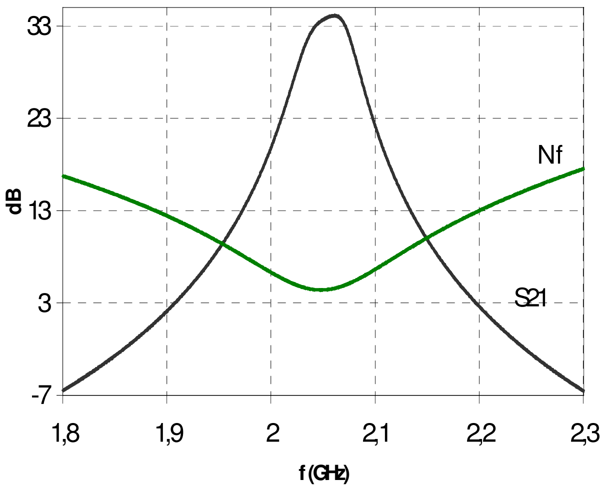

Fig. 7 S21 and NF parameters

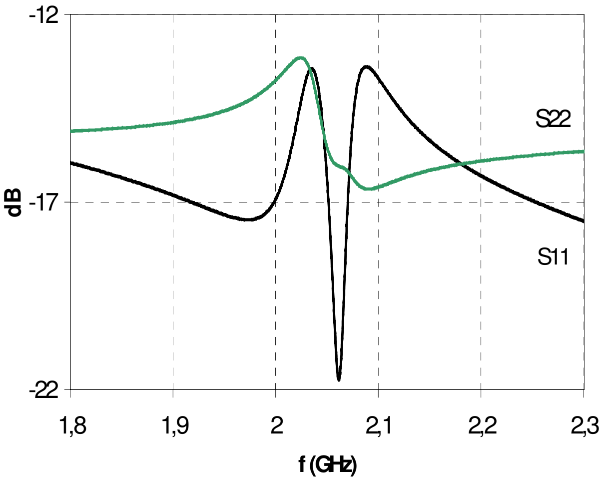

Fig. 8 S11 and S22 parameters

Differential probes have been used to characterise the circuit. Agilent Tech. E5071B network analyser is used for mixed-mode method measurements for which the 16 classical scattering parameters are converted to the so called mixed parameters. They address differential and common mode as well as the conversion between the two modes. Tab. 2 sums up the most important data in three cases referred by plot (1) to (3).

Mixed mode	Plot (1) (Simulation)	Plot (2) (measure)	Plot (3) (measure)
	F_0=2.05Ghz Vcc=2.7 V Vf=2 V	F_0=2.25Ghz same Vcc and Vf as simulation	F_0=2.05Ghz Vf=2.8 V
Sdd11	-23 dB	-4 dB	-8.35 dB
Sdd12	-60 dB	-45 dB	-60 dB
Sdd21	+34 dB	+25.7 dB	+23 dB
Sdd22	-15 dB	-6 dB	-7 dB
Scc11	-2 dB	-4 dB	-4 dB
Scc12	-62 dB	-45 dB	-45 dB
Scc21	-38 dB	-12 dB	-16.5 dB
Scc22	-16 dB	-16 dB	-16.5 dB
Scdxx	< -10 dB	< -10 dB	< -10 dB
Sdcxx	< -10 dB	< -10 dB	< -10 dB

Tab. 2 Mixed mode scattering parameters

Plot (1) in Fig 9-a,b,c,d,e represents the extracted Cadence simulated response with 2.7 V power supply and voltage control frequency Vf of 2 V. Plot (2) represents measurements with the same power supply and Vf simulated conditions. Plot (3) represents measurements with increased potential of Vf = 2.8 V. During measurements, power supplying the right branch (Fig.5) is increased by 0.15 V with respect to other side due to a fair dissymmetry in the circuit layout.

The circuit shows in plot (2) a purely differential transmission scattering parameter Sdd21 with a frequency shift to 2.25 GHz and lower gain of 25.7 dB instead of the expected 34 dB as seen on Fig 9-a. This shift is probably due to inductor block modelling problem and couplings with active elements. In the third case plot (3), the circuit shows an interesting frequency tuning with different polarisation Vf.

In Tab. 2, Sdd11 and Sdd22 parameters are respectively -4 dB and -6 dB for plot (2) and -8.35 dB and -7 dB for plot (3) respectively. These values give an idea on input and output matching for a purely differential mode. Common mode scattering parameters (like Scc21) show small values thus verifying a good rejection of this mode. The eight last parameters express differential-common and common-differential conversions. They are less than -10 dB, again confirming the circuit symmetry.

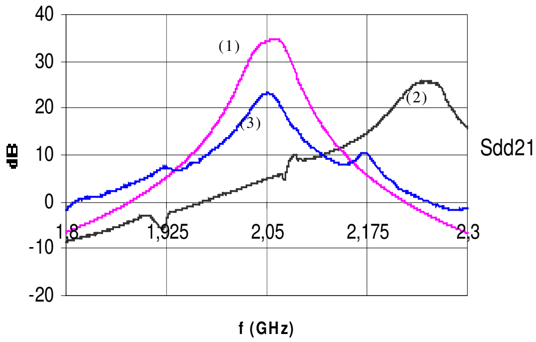

Fig. 9-a Sdd21

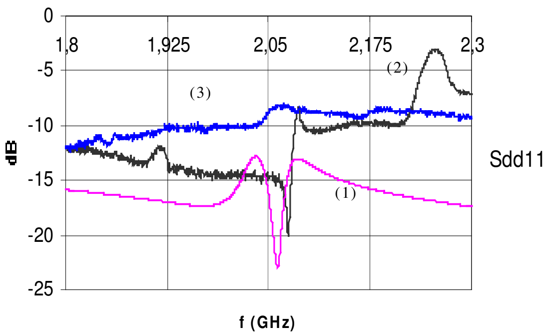

Fig. 9-b Sdd11

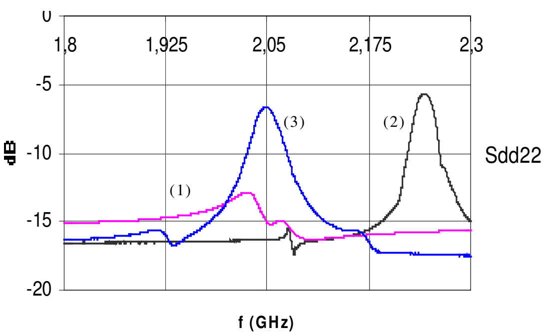

Fig. 9-c Sdd22

ACKNOWLEDGEMENT

The authors wish to acknowledge R&D department of Philips Company at Caen for their assistance and the realisation of the chip.

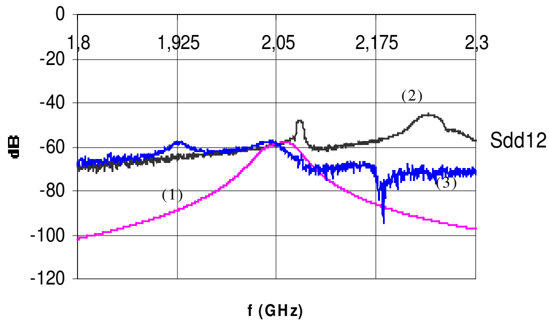

Fig. 9-d Sdd12

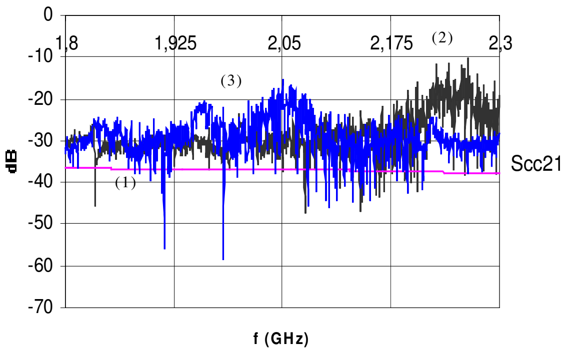

Fig.9-e Scc21

REFERENCES

[1] D. Szmyd, R. Brock, N. Bell, S. Harker, G. Patrizi, J. Fraser, R. Dondero, “QUBIC4 : a silicon RF-BiCMOS technology for wireless communication Ics”, Proceedings of the 2001 bipolar/BiCMOS Circuits and Technology Meeting, pp.60-63

[2] A.N.Mohieldin,, Sanchez-Sinencio, and Silva-Marinez, J., "A 2.7V, 1.8GHz, 4th Order Tunable LC Bandpass Filter with ±0.25dB Passband Ripple," European Solid-State Circuits Conference, pp. 427-430, Florence, Italy, September 27, 2002.

[3] R. Duncan, K. W. Martin, and A. Sedra, “A Q-enhanced active RLC bandpass filter,” IEEE Trans. Circuits Syst. II, vol. 44, pp. 341–346, May 1997.

[4] W. B. Kuhn, F. W. Stephenson, and A. Elshabini-Riad, “A 200-MHz CMOS Q-enhanced LC bandpass filter,” IEEE J. Solid-State Circuits, vol. 31, pp. 1112–1122, Aug. 1996.

[5] W. B. Kuhn, N. K. Yanduru, and A. S. Wyszynski, “Q-enhanced LC bandpass filters for integrated wireless applications,” IEEE Trans. Microwave Theory Tech., vol. 46, pp. 2577–2586, Dec. 1998.

[6] D. Li and Y. Tsividis, “A 1.9-GHz Si active LC filter with on-chip automatic tuning,” in IEEE Int. Solid-State Circuits Conf. Dig. Tech. Papers, 2001, pp. 368–369.

[7] A. M. Niknejad and R. G. Meyer, “Analysis, design, and optimization of spiral inductors and transformers for Si RF ICs,” IEEE J. Solid-State Circuits, vol. 33, pp. 1470–1481, Oct. 1998.

[8] A. I. Zverev, “Handbook of Filter Synthesis”. New-York, Wiley, 1967.